ENGINEERING JOURNAL

Article

A Comparative Study of Different Al-Based Solid Acid Catalysts for Catalytic Dehydration of Ethanol

Tanutporn Kamsuwan and Bunjerd Jongsomjit*

Center of Excellence on Catalysis and Catalytic Reaction Engineering, Department of Chemical Engineering, Faculty of Engineering, Chulalongkorn University, Bangkok 10330, Thailand
*E-mail: bunjerd.j@chula.ac.th (Corresponding author)

Abstract. In this present study, the catalytic dehydration of ethanol over three different Al-based solid acid catalysts including H-beta zeolite (HBZ), modified H-beta zeolite with γ-Al_2O_3 (Al-HBZ) and mixed γ- χ phase of Al_2O_3 (M-Al) catalysts was investigated. The ethanol dehydration reaction was performed at temperature range of 200 to 400°C. It revealed that all catalysts exhibited higher ethanol conversion with increased temperatures. At low temperatures (ca. 200 to 250°C), diethyl ether (DEE) was obtained as a major product for all catalysts. However, with increased temperatures (ca. 300 to 400°C), ethylene was a major product. Among all catalysts, HBZ exhibited the highest ethanol conversion giving the ethylene yield of 99.4% at 400°C. This can be attributed to the largest amount of weak acid sites present in HBZ, which is related to the Brønsted acid. It should be mentioned that HBZ also rendered the highest catalytic activity for every reaction temperature. As the results, HBZ catalyst is promising to produce ethylene and DEE from ethanol, which is considered as cleaner technology.

Keywords: Ethylene, diethyl ether, ethanol dehydration, Al-based catalyst, zeolite.

ENGINEERING JOURNAL Volume 20 Issue 3
Received 18 September 2015
Accepted 6 January 2016
Published 19 August 2016
Online at http://www.engj.org/
DOI:10.4186/ej.2016.20.3.63

DOI:10.4186/ej.2016.20.3.63

1. Introduction

Ethylene is an important chemical in petrochemical industries, which is the most widely used as feedstock to produce ethylene oxide (EO) and polymers such as polyethylene (PE), polyethylene terephthalate (PET), and polyvinylchloride (PVC) [1–3]. At present, ethylene is mainly produced by thermal cracking of petroleum-based products such as naphtha. This process consumes intensive high energy generating large amounts of CO_2 greenhouse gas emissions. Therefore, the catalytic dehydration of ethanol to ethylene is an alternative promising way to obtain the reduction of CO_2 emission, low production cost and energy consumption [3, 4] since it is cleaner technology than the conventional process. There are many solid acid catalysts used for ethanol dehydration to ethylene, which are efficient in catalyzing the dehydration of ethanol. These catalysts include the supported phosphoric acid, alumina, silica-alumina, heteropolyacid catalysts and zeolites [5, 6]. Furthermore, different transition metal catalysts such as titanium oxides, magnesium oxides, cobalt oxides, chromium oxide and silver salt of tungstophosphoric acid [7, 8] were also investigated for the catalytic dehydration of ethanol. The catalytic activity for dehydration of ethanol could be correlated to the number of strong Brønsted acid sites in catalyst [9].

In recent years, alumina (Al_2O_3) and zeolites (alumino-silicate materials) have been used as solid acid catalysts for ethanol dehydration. H-ZSM-5 zeolite has a good performance at lower reaction temperature having higher ethylene yield, but it easily deactivates by coke formation during the reaction due to its smaller pore size and strong acidic properties[5, 10]. Using alumina and/or other types of zeolite or modified H-ZSM-5 as catalysts instead of H-ZSM-5 should be preferred to avoid the coke formation during the process of ethanol dehydration [11–13]. The physicochemical properties of alumina catalysts depend on the methods of preparation and calcination conditions. There are many methods to synthesize alumina catalysts such as solvothermal synthesis, sol-gel synthesis, flame spray pyrolysis, precipitation, emulsion evaporation, microwave synthesis, hydrothermal synthesis and heat treatment of aluminium hydroxides such as boehmite and gibbsite. The solvothermal and sol-gel methods are commonly used for synthesis of alumina [14]. The γ-Al_2O_3 and mixed γ-χ phase Al_2O_3 catalysts were also investigated for this reaction because they exhibit high thermal stability, fine particle size, high surface area, inhibit side reaction and high acidity, which is enough to produce ethylene via ethanol dehydration. It was also found that crystal structures, grain sizes and morphologies can be controlled by process conditions such as solute concentration, reaction temperature, reaction time and the type of solvent [14, 15]. However, there have been no reports of the ethanol dehydration to ethylene over H-beta zeolite (HBZ), which is microporous zeolite having high surface area, high thermal stability and high acidity. Moreover, H-beta zeolite exhibits larger pore size than H-ZSM-5. Hence, it is expected to produce hydrocarbon with less coke deposition due to higher diffusivity in the pore [16].

In this work, we report the characteristics and catalytic properties of different Al-based catalysts including HBZ, modified H-beta zeolite with γ-Al_2O_3 (Al-HBZ) and mixed γ-χ phase Al_2O_3 (M-Al) catalysts over the catalytic ethanol dehydration. The catalysts were characterized using various techniques such as X-ray diffraction (XRD), N_2physisorption, scanning electron microscopy (SEM) and energy dispersive X-ray spectroscopy (EDX), and temperature-programmed desorption of ammonia (NH_3-TPD). The catalytic properties were measure towards the gas-phase ethanol dehydration using a fixed-bed flow microreactor to measure the ethanol conversion and product distribution.

2. Experimental

2.1. Materials

The commercial HBZ used in this study was purchased from Tosoh Corporation. The typical structure of HBZ is shown in Scheme 1. Aluminium isopropoxide: AIP (98% from Sigma-Aldrich chemical company, Inc.), toluene (99% Merck Company Ltd.), 1-butanol (99% Merck company Ltd.), methanol (Merck company Ltd.), ethanol (99.99% Merck company Ltd.), ultra-high purity nitrogen gas [99.99% Linde (Thailand) Public Company Ltd.], hydrochloric acid (37.7% hydrochloric acid from Sigma-Aldrich chemical company, Inc.) were employed.

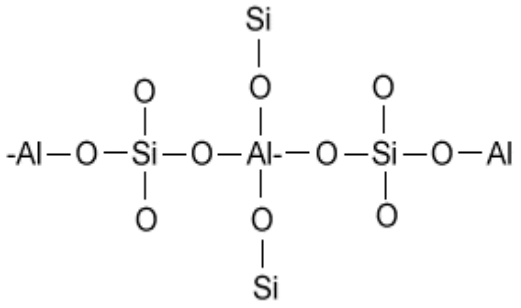

Scheme 1. Typical structure of H-beta zeolite (HBZ) [17].

2.2. Preparation of Al-based Catalysts

Besides the HBZ catalyst, other two Al-based catalysts were used and prepared from different methods. The mixed γ-χ Al_2O_3 (M-Al) was prepared by the solvothermal method as reported by Janlamool and Jongsomjit [18]. The modified H-beta zeolite with γ-Al_2O_3(Al-HBZ) was prepared by the modified sol-gel method. First, aluminium isopropoxide precursor was hydrolyzed in solution of ethanol and deionized water with volume ratio of 1:1 by stirring at 80ºC for 1 h and then at 90ºC for 15 minutes. After that, the HBZ was added into the solution with HBZ to Al weight ratio of 1:3.Subsequently, hydrochloric acid was added to the solution, which was stirred at 90ºC for 10 h with the controlled pH of 2.5. After this step, the product became viscous. The formed gel was dried overnight at 110°C and calcined at 550°C under air flow for 2 h to obtain the Al-HBZ catalyst.

2.3. Catalyst Characterization

All catalysts were characterized by several techniques as follows:

X-ray diffraction (XRD): XRD was performed to determine the bulk crystalline phases of sample. It was conducted using a SIEMENS D-5000 X-ray diffractometer with CuK_α (λ = 1.54439 Å). The spectra were scanned at a rate of 2.4° min^{-1} in the range of 2 theta = 10 to 90°.

N_2physisorption: Measurement of BET surface area, average pore diameter and pore size distribution were determined by N_2physisorption using a Micromeritics ASAP 2000 automated system.

Temperature-programmed desorption of ammonia (NH_3-TPD): The acid properties of catalysts were investigated by NH_3-TPD using Micromeritics Chemisorb 2750 pulse chemisorption system.

Scanning electron microscopy (SEM) and energy dispersive X-ray spectroscopy (EDX): SEM and EDX were used to investigate the morphology and elemental distribution of catalysts, respectively using Hitashi mode S-3400N. Micrographs were taken at the accelerating voltage of 30 kV and magnification ranging from 1,000 to 10,000 and the resolution of 3 nm. The SEM was operated using the secondary scattering electron (SE) mode. EDX was performed using Apollo X Silicon Drift Detector Series by EDAX. Before the SEM observation, the sample was conductive to prevent charging by coating with platinum particle under the ion sputtering device.

2.4. Reaction Test

The dehydration of ethanol was carried out in a fixed-bed continuous flow microreactor made from a borosilicate glass with an inside diameter of 0.7 cm and length of 33 cm. The reaction system is shown in Scheme 2. In the experiment, 0.01 g of packed quartz wool and 0.05 g of catalyst were loaded into the reactor. Then, the catalyst was pretreated in argon (60ml/min) at 200°C for 1 h under atmospheric pressure. The liquid ethanol was vaporized in a flowing of argon by controlled injection with a single syringe pump at a constant flow rate of ethanol 1.45 ml/h [WHSV = 22.9 ($g_{ethanol}g_{cat}^{-1}$) h^{-1}].The reaction was carried out at temperature ranging from 200 to 400°C by feeding the vaporized ethanol into the reactor. The reaction was carried out at each temperature for 1 h. The products were analyzed by a Shimadzu GC8A gas chromatograph with flame ionization detector (FID) using capillary column (DB-5). Nitrogen (pressure of 260 kPa) was used as carrier gas in GC using the temperature of injector and detector at 150°C

2.5. Calculation

In this work, the ethanol conversion (X_{EtOH}), ethylene selectivity (S_E), diethyl ether selectivity (S_{DEE}), ethylene yield (Y_E) and diethyl ether yield (Y_{DEE}) are defined as follows:

$$X_{EtOH} = \frac{n_{EtOH,0} - n_{EtOH,1}}{n_{EtOH,0}} \times 100 \quad (1)$$

$$S_E = \frac{n_{E,1}}{\sum n_{i,1}} \times 100 \quad (2)$$

$$S_{DEE} = \frac{2n_{DEE,1}}{\sum n_{i,1}} \times 100 \quad (3)$$

$$Y_E = \frac{S_E \times X_{EtOH}}{100} \quad (4)$$

$$Y_{DEE} = \frac{S_{DEE} \times X_{EtOH}}{100} \quad (5)$$

where $n_{EtOH,0}$ and $n_{EtOH,1}$ are defined as the molar flow rate (mmol/min) of ethanol in feed and in products, respectively; $n_{E,1}$, $n_{DEE,1}$, and $\sum n_{i,1}$ are defined as the molar flow rate of ethylene, diethyl ether and total products, respectively [4, 19].

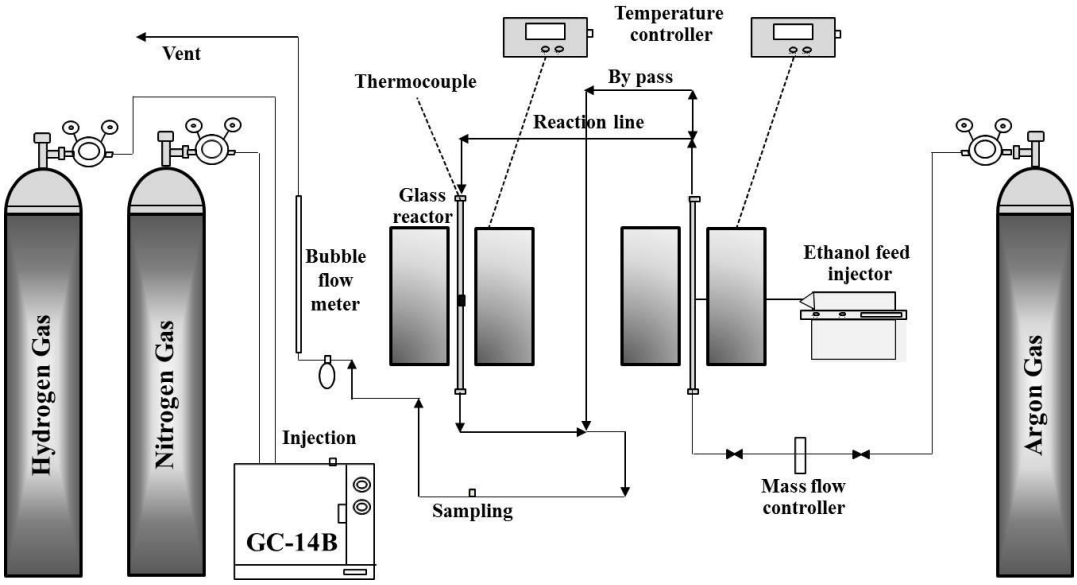

Scheme 2. Ethanol reaction system.

3. Results and Discussion

3.1. Catalyst Characterization

The XRD patterns of different catalysts are shown in Fig. 1. The specific sharp peaks of HBZ catalyst consist of 2θ at 14.6and 22.4° [16, 20]. The characteristic peaks of pure γ-Al_2O_3 are 46 and 67°[18]. When adding γ-Al_2O_3 into HBZ to obtain the Al-HBZ catalyst, XRD peaks were appeared at 14.6, 22.4 (HBZ), 46 and 67° (γ-Al_2O_3). It indicated that the main structure of HBZ did not alter with Al addition. It was appeared that the intensity of characteristic peak (22.4°) for HBZ decreased with Al addition suggesting that the lower crystallinity of Al-HBZ was obtained. For the M-Al catalyst, the XRD peaks were appeared at 43, 46and 67°, which can be assigned to the presence of γ-Al_2O_3 (46and 67°) coupled with χ- Al_2O_3 (43°) as also reported by Janlamoon and Jongsomjit [18].

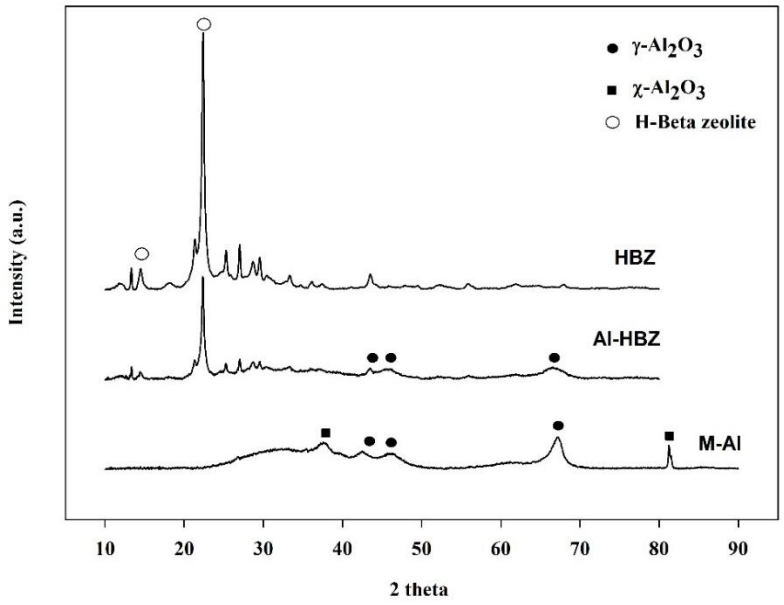

Fig. 1. XRD patterns of all catalysts.

The BET surface area (S_{BET}) of catalysts is listed in Table 1. The HBZ catalyst exhibits the largest surface area of 522 m^2/g. With Al addition, the decreased surface area (306 m^2/g) was evident for the Al-HBZ catalyst due to the pore blockage of Al in HBZ. The surface area of M-Al catalyst was 195 m^2/g. The large surface area helps more opportunities for reactants to contact and react, which would adjust the catalytic activity for ethanol dehydration [4].

Table 1. Properties of catalysts.

Catalyst	Pore size diameter (nm)	BET Surface Area S_{BET} (m^2/g)	NH_3 desorption (μmol NH_3/g)		Total acidity (μmol NH_3/g)
			Weak	Medium to strong	
HBZ	2.2	521.6	844.8	672.5	1517.3
Al-HBZ	3.4	305.9	813.3	731.6	1544.9
M-Al	9.0	195.4	268.7	510.0	778.6

The N_2 adsorption-desorption isotherms for all catalysts are shown in Fig. 2. The pore structure of HBZ exhibited the characteristic of microporous structure according to type I classified by IUPAC (International Union of Pure and Applied Chemistry). After the introduction of Al to obtain Al-HBZ, the characteristic of type I was still observed. However, a small hysteresis loop also occurred at P/P_o around 0.4 to 0.8 indicating the presence of a small portion of mesoporous structure regarding type IV with introduction of Al. This is corresponding to the decreased surface area of Al-HBZ compared to HBZ. The M-Al showed the pore structure of mesoporous material according to type IV indicating the lowest surface area among other two catalysts.

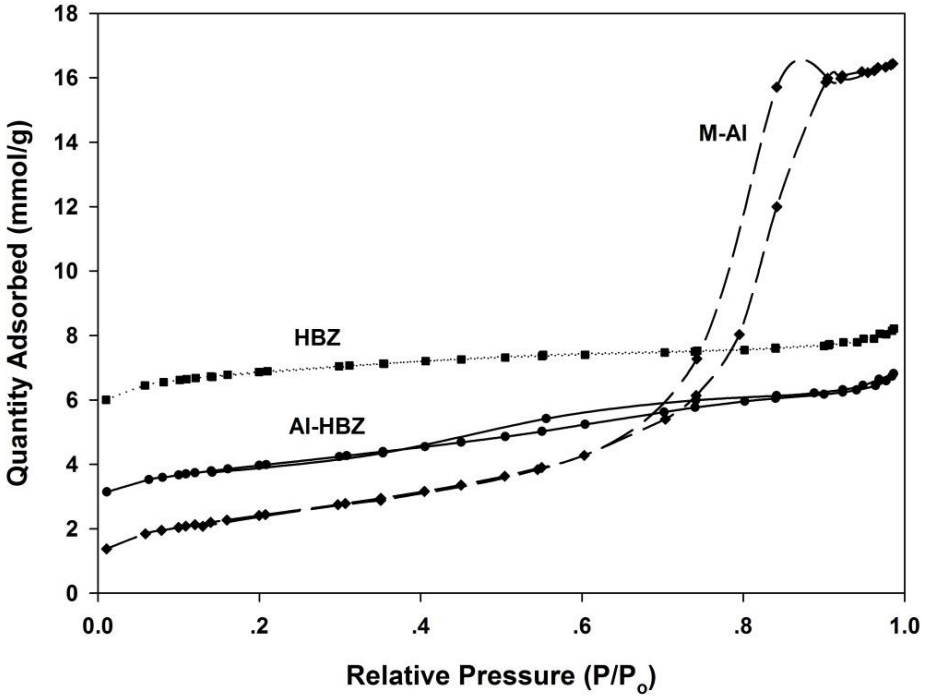

Fig. 2. The N_2 adsorption-desorption isotherms for all catalysts.

Figure 3 shows the pore size distribution of catalysts, which are related to the pore structure as discussed from Fig. 2. The average pore size (Table 1) of HBZ was ca.2 nm (micropore). The average pore size of M-Al was ca.9 nm (mesopore), whereas the Al-HBZ exhibited mainly microporous structure with only a small portion of mesoporous structure as also mentioned above. The difference in pore size diameter and S_{BET} affected the observed productivity in this reaction because the small pore size and high S_{BET} may decrease higher hydrocarbon and byproducts leading to increasing of main product selectivity and ethanol conversion. Moreover, the high S_{BET} would affect to the increased catalytic activity for ethanol dehydration [4].

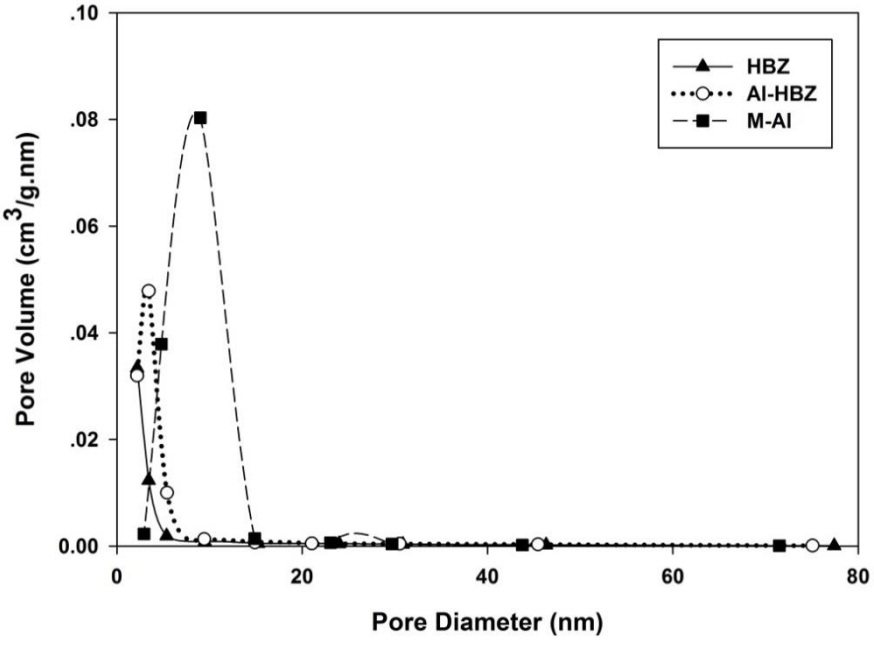

Fig. 3. Pore size distribution for all catalysts.

The morphology of catalysts was determined by SEM as shown in Fig. 4. It can be observed that morphologies of both HBZ and Al-HBZ were similar spheroidal, but Al-HBZ had a rougher surface than HBZ due to Al deposition. The M-Al showed different morphology with more roughness.

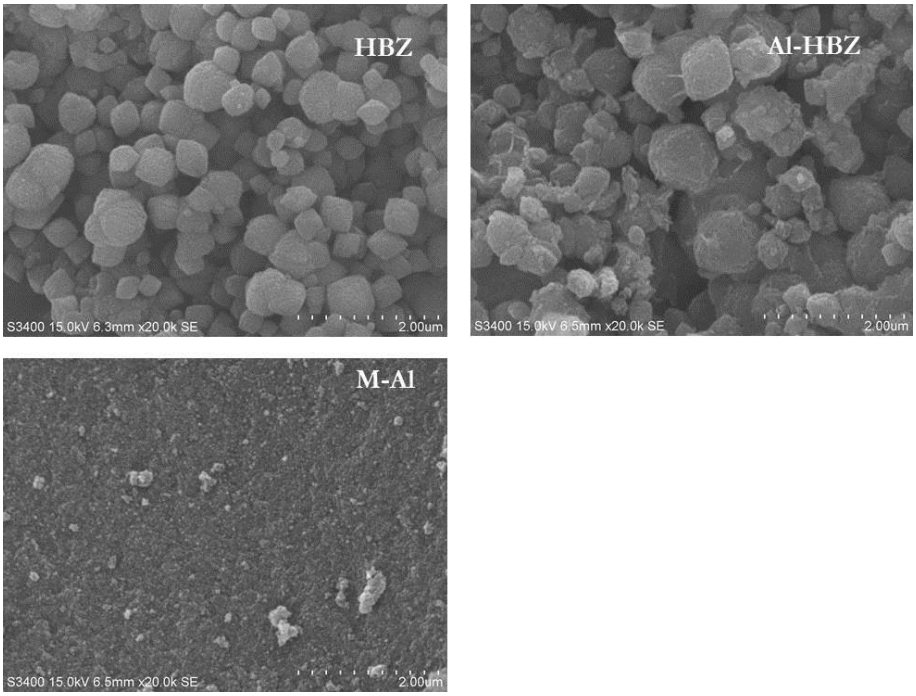

Fig. 4. SEM images of all catalysts.

The EDX analysis was used to quantitatively measure the amounts of elemental composition on the catalyst surface. The results are illustrated in Table 2. It revealed the chemical composition of each catalyst. The amounts of Al present at surface were in the range of M-Al > Al-HBZ > HBZ, which were reasonable. In other words, the Si/Al ratio of HBZ was the highest. The decreased Si/Al ratio is perhaps related to the decrease in weak acid sites, but increased strong acid sites as well as increased total acidity [21]. Thus, the acid properties of catalysts were determined using NH_3-TPD.

Table 2. Elemental composition obtained from EDX.

Catalyst	Element						
	% Weight				% Atom		
	Al	Si	O	Si/Al	Al	Si	O
HBZ	3.26	44.95	51.78	13.79	2.44	32.28	65.28
Al-HBZ	32.1	22.59	45.31	0.70	24.55	16.67	58.68
M-Al	61.06	-	38.94	-	48.18	-	51.82

The NH_3-TPD profiles (Fig. 5) of all catalysts were similar consisting of two groups of desorption peaks. The desorption peaks at low temperature below 250°C are assigned to weak acid sites, whereas those above 400°C are strong acid sites. The number of acid site on catalyst can be calculated by integration of desorption area of ammonia according to the Gauss curve fitting method. The amount of acidity of catalysts is also displayed in Table 1. It was found that HBZ had the highest amount of weak acid sites. The addition of Al into HBZ resulted in decreased amount of weak acid site, but increased moderate to strong acid sites as well as total acidity. This can be attributed to the addition of Al possibly alter the acid distribution with different Si/Al ratios of catalysts [21]. Furthermore, the slight difference in total acidity of HBZ and Al-HBZ perhaps results from only slightly different Si/Al ratios. However, the addition of alumina into H-beta zeolite may result in slightly increased amount of medium to strong acid site [22]. However, the amount of weak acid site, moderate to strong acid site and total acid site of M-Al were the

lowest among other two catalysts. It was reported that the weak acid site is essential for the catalytic dehydration of ethanol to ethylene [4, 5, 22, 23]. Thus, the presence of large amount of weak acid would be beneficial to enhance the catalytic activity.

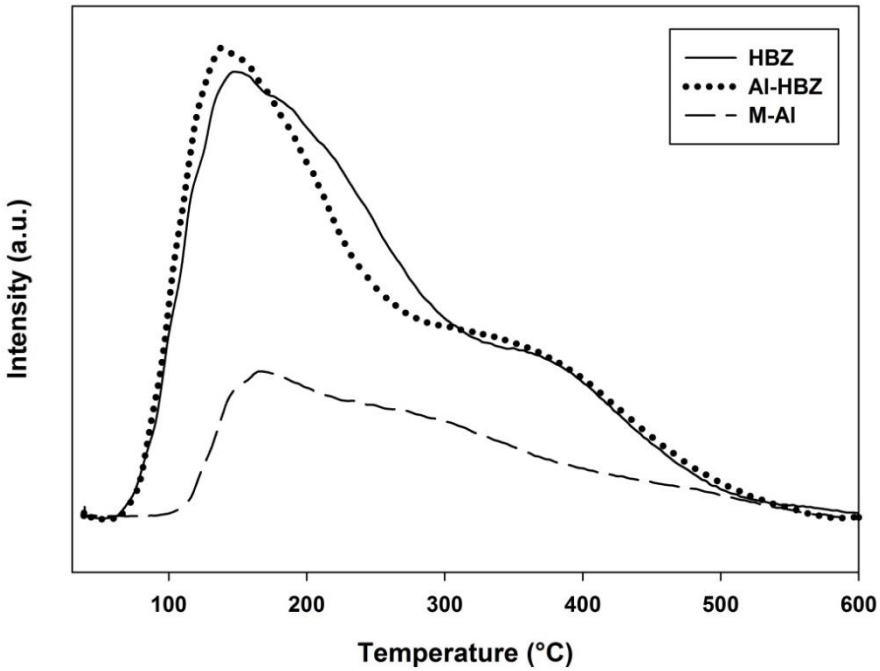

Fig. 5. NH_3-TPD profiles of all catalysts.

3.2. Catalytic Properties

It is known that ethanol dehydration reaction has two competitive ways occurred [4] as follows:

$$C_2H_5OH \rightarrow C_2H_4 + H_2O \qquad +44.9 \text{ kJ/mol} \qquad (6)$$

$$2C_2H_5OH \rightarrow C_2H_5OC_2H_5 + H_2O \qquad -25.1 \text{ kJ/mol} \qquad (7)$$

The first reaction (6) is dehydration of ethanol to ethylene (endothermic reaction), while the second one (7) is side reaction to produce DEE (exothermic reaction). DEE is produced in significant quantities at low temperature. However, ethylene is obtained via ethanol dehydration at high temperatures. The Mechanism of dehydration reaction to ethylene and DEE is shown in Schemes 3 and 4, respectively. Figure 6 shows the ethanol conversion at temperature range of 200 to 400°C. Ethanol conversion apparently increased with increased temperature. It was found that the HBZ exhibited the highest conversion of ethanol among other two catalysts for all reaction temperature. This can be attributed to the large amount of weak acid sites present in HBZ catalyst. The ethanol conversion for Al-HBZ and M-Al was found to have a similar trend with that of HBZ, where the conversion increased with increasing reaction temperature. However, the conversion obtained from HBZ was the highest.

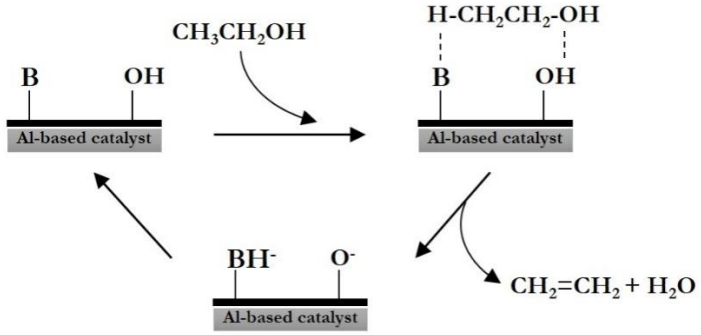

Scheme 3. Ethanol dehydration to ethylene at base (B) and Brønsted acid(OH) catalyst sites [24].

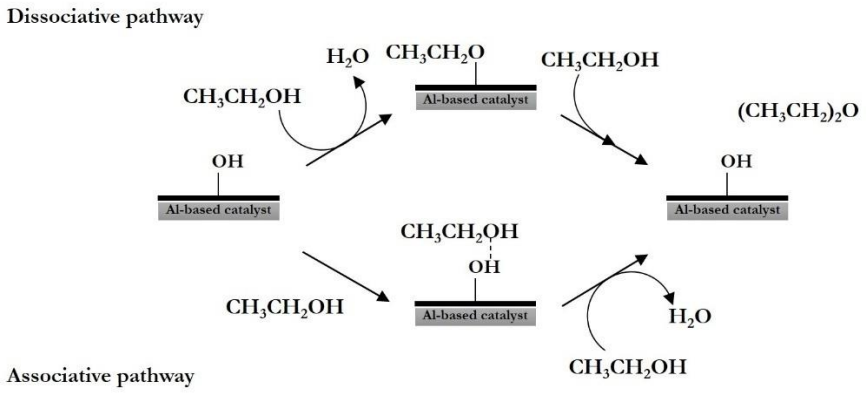

Scheme 4. Ethanol dehydration to DEE [24].

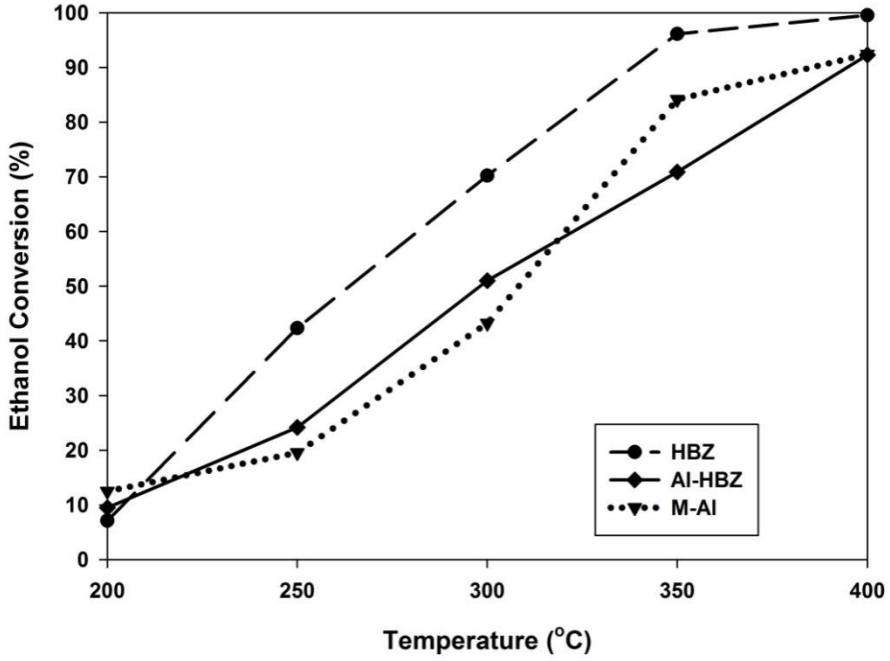

Fig. 6. Ethanol conversion for all catalysts.

The ethylene selectivity of catalysts is shown in Fig. 7. For all catalysts, the ethylene selectivity increased with increasing reaction temperature. The HBZ catalyst produced more ethylene than other two catalysts. However, at 400°C, the selectivity to ethylene for all catalysts was almost equal.

DOI:10.4186/ej.2016.20.3.63

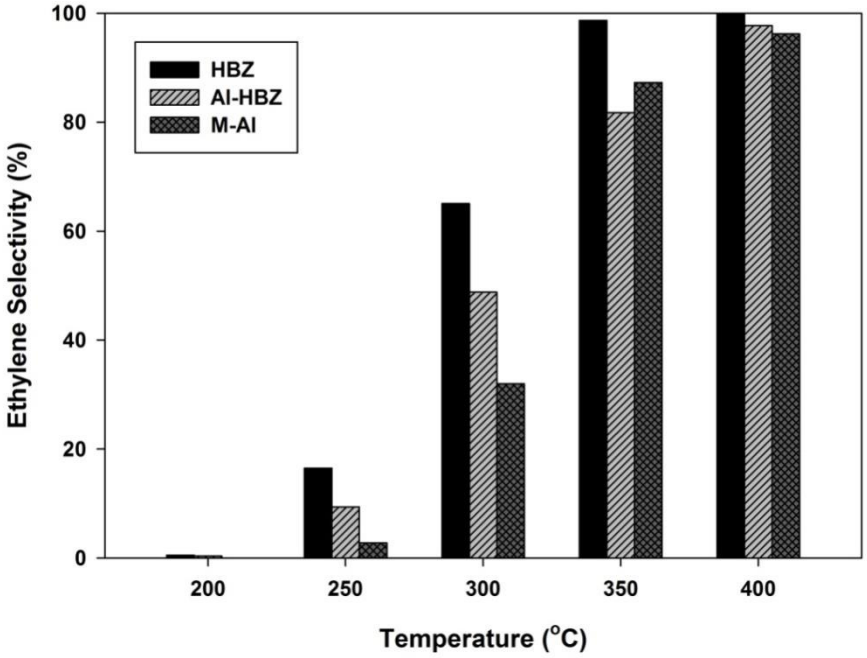

Fig. 7. Ethylene selectivity for all catalysts.

Besides ethylene, DEE is also obtained, especially at low reaction temperature. The DEE selectivity is shown in Fig. 8. It can be observed that at 200°C, all catalysts produced only DEE. However, at this temperature, the ethanol conversion was extremely low. Hence, the DEE yield (product of ethanol conversion and DEE selectivity) was quite low. It was found that the M-Al catalyst exhibited slightly higher DEE selectivity than other two catalysts.

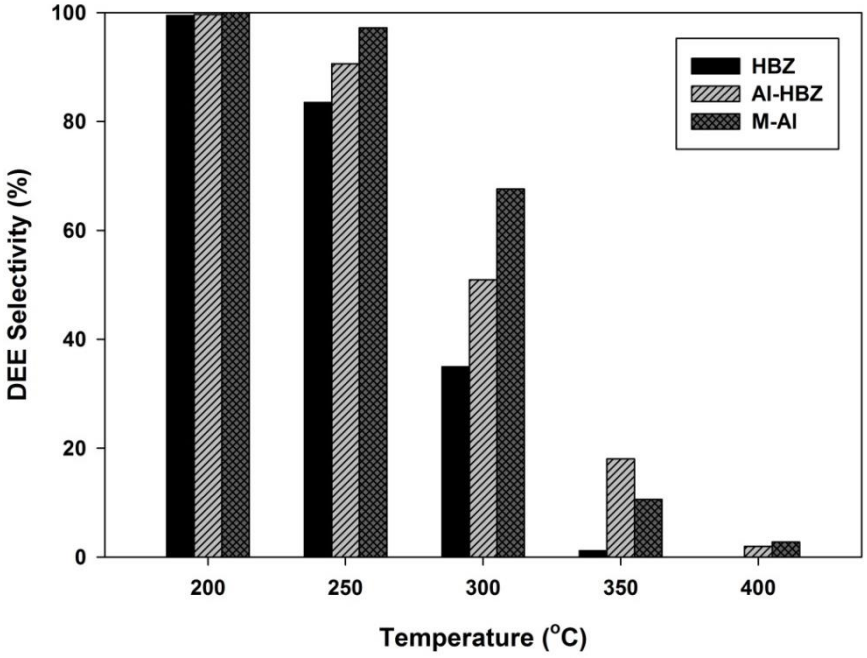

Fig. 8. DEE selectivity for all catalysts.

In order to compare the product yields obtained from catalysts. The product yields were calculated at different temperatures as shown in Table 3. Considering for ethylene selectivity, the highest ethylene yield

was obtained at 400°C indicating that high catalytic activity as well as ethanol conversion is the highest when compared with low temperature reaction. The increase in ethanol conversion results in increased product yield. At 400°C, the ethylene yield increased in the range of HBZ > Al-HBZ > M-Al. The DEE selectivity is also interesting. It can be observed that the highest DEE yield (35.3%) was obtained from the HBZ catalyst at 250°C. The low DEE yield was caused by low conversion. In order to improve the DEE yield, the chemical promoter is perhaps necessary. Chen et al. studied the addition of some chemical promoters to improve the catalytic dehydration. The chemical promoters used for this reaction such as titania, niobia, molybdenum oxide and silica were investigated [19, 25–27].

Table 3. Product yield of all catalysts

Catalyst	Ethylene yield (%)					DEE yield (%)				
	200 °C	250 °C	300 °C	350 °C	400 °C	200 °C	250 °C	300 °C	350 °C	400 °C
HBZ	0.0	7.0	45.7	94.8	99.4	7.1	35.3	24.5	1.1	0.0
Al-HBZ	0.0	2.3	24.9	57.9	90.2	9.5	21.9	26.0	12.8	1.8
M-Al	0.0	0.5	13.8	73.4	88.9	12.5	19.0	29.2	8.9	2.5

Table 4. Comparison of catalysts for ethylene synthesis and their catalytic ability.

Catalyst	Surface area (m^2/g)	Reaction temperature (°C)	Ethanol conversion (%)	Ethylene selectivity (%)	Ref.
HBZ	522	200-400	7-100	1-100	This work
Al-HBZ	306	200-400	9-92	0-98	This work
M-Al	195	200-400	12-92	0-96	This work
H-ZSM-5	366	400	99	10	[13]
20HP-ZSM-5	74	250-450	25-100	3-98	[13]
γ-Al_2O_3	204	400-550	70-100	40-95	[19]
TiO_2/γ-Al_2O_3	187	360-550	70–100	50–99	[19]
SAPO-34	300	500	100	100	[28]
ZS(25)-HS-4	276	500	100	27	[28]
ZS(25)-MM-4	352	500	100	24	[28]

Moreover, there were summarized reports of catalytic ability for ethanol dehydration to ethylene over various catalysts (Table 4). It is shown that HBZ, Al-HBZ and M-Al catalysts in this work are comparable to those of typical and modified catalysts. Ramesh et al. and Duan et al. studied structure and reactivity of modified H-ZSM-5 catalysts for ethanol dehydration. They found that the highest surface area was obtained by unmodified H-ZSM-5 and testing of catalytic activity at 250-500°C. Then, the result showed that ethanol conversion and ethylene selectivity of modified H-ZSM-5 were lower than that of HBZ for this work. It can be concluded that HBZ exhibited higher catalytic activity than their catalysts [13, 28]. In addition, Chen et al. investigated the modification effects of TiO_2-doped on alumina catalysts packed in microreactor. Their results showed that the catalytic activity of their catalyst was lower than that of Al-HBZ and M-Al catalysts at the same reaction temperature [19]. Thus, the HBZ is practical to be applied for the ethanol dehydration to ethylene.

4. Conclusion

Among all three Al-based catalysts in this study, the HBZ catalyst is the most effective to convert ethanol into ethylene with ca. 99% of ethylene yield (at high temperature, i.e. 400°C) and DEE with ca. 35.3% of DEE yield (at low temperature, i.e. 250°C). This is attributed to the high amount of weak acid sites present in the HBZ catalyst. Although, no deactivation of catalyst was found at 400°C, the stability test towards time on stream (TOS) should be further investigated in future work. Considering the production of DEE from ethanol at low temperature (250°C), it is possible to use the HBZ catalyst.

Acknowledgement

The authors thank the Thailand Research Fund (TRF), the National Research Council of Thailand (NRCT) and Ratchadaphiseksomphot Endowment Fund (2015) of Chulalongkorn University (CU-58-027-AM) for financial support of this project.

References

[1] A. P. Kagyrmanova, V. A. Chumachenko, V. N. Korotkikh, V. N. Kashkin, and A. S. Noskov, "Catalytic dehydration of bioethanol to ethylene: Pilot-scale studies and process simulation," *Chemical Engineering Journal,* vol. 176-177, pp. 188-194, 2011.

[2] J. Bedia, R. Barrionuevo, J. Rodríguez-Mirasol, and T. Cordero, "Ethanol dehydration to ethylene on acid carbon catalysts," *Applied Catalysis B: Environmental,* vol. 103, no. 3-4, pp. 302-310, 2011.

[3] V. V. Bokade, and G. D. Yadav, "Heteropolyacid supported on montmorillonite catalyst for dehydration of dilute bio-ethanol," *Applied Clay Science,* vol. 53, no. 2, pp. 263-271, 2011.

[4] Y. Chen, Y. Wu, L. Tao, B. Dai, M. Yang, Z. Chen, and X. Zhu, "Dehydration reaction of bio-ethanol to ethylene over modified SAPO catalysts," *Journal of Industrial and Engineering Chemistry,* vol. 16, no. 5, pp. 717-722, 2010.

[5] Q. Sheng, K. Ling, Z. Li, and L. Zhao, "Effect of steam treatment on catalytic performance of HZSM-5 catalyst for ethanol dehydration to ethylene," *Fuel Processing Technology,* vol. 110, pp. 73-78, 2013.

[6] L. Matachowski, M. Zimowska, D. Mucha, and T. Machej, "Ecofriendly production of ethylene by dehydration of ethanol over $Ag_3PW_{12}O_{40}$ salt in nitrogen and air atmospheres," *Applied Catalysis B: Environmental,* vol. 123-124, pp. 448-456, 2012.

[7] T. Zaki, "Catalytic dehydration of ethanol using transition metal oxide catalysts," *Journal of Colloid and Interface Science,* vol. 284, no. 2, pp. 606-613, 2005.

[8] T. K. Phung, R. Radikapratama, G. Garbarino, A. Lagazzo, P. Riani, and G. Busca, "Tuning of product selectivity in the conversion of ethanol to hydrocarbons over H-ZSM-5 based zeolite catalysts," *Fuel Processing Technology,* vol. 137, pp. 290-297, 2015.

[9] A. Rahmanian, and H. S. Ghaziaskar, "Continuous dehydration of ethanol to diethyl ether over aluminum phosphate–hydroxyapatite catalyst under sub and supercritical condition," *The Journal of Supercritical Fluids,* vol. 78, pp. 34-41, 2013.

[10] F. Wang, M. Luo, W. Xiao, X. Cheng, and Y. Long, "Coking behavior of a submicron MFI catalyst during ethanol dehydration to ethylene in a pilot-scale fixed-bed reactor," *Applied Catalysis A: General,* vol. 393, no. 1-2, pp. 161-170, 2011.

[11] N. Zhan, Y. Hu, H. Li, D. Yu, Y. Han, and H. Huang, "Lanthanum–phosphorous modified HZSM-5 catalysts in dehydration of ethanol to ethylene: A comparative analysis," *Catalysis Communications,* vol. 11, no. 7, pp. 633-637, 2010.

[12] J. Bi, X. Guo, M. Liu, and X. Wang, "High effective dehydration of bio-ethanol into ethylene over nanoscale HZSM-5 zeolite catalysts," *Catalysis Today,* vol. 149, no. 1-2, pp. 143-147, 2010.

[13] K. Ramesh, L. Hui, Y. Han, and A. Borgna, "Structure and reactivity of phosphorous modified H-ZSM-5 catalysts for ethanol dehydration," *Catalysis Communications,* vol. 10, no. 5, pp. 567-571, 2009.

[14] C. Meephoka, C. Chaisuk, P. Samparnpiboon, and P. Praserthdam, "Effect of phase composition between nano γ- and χ-Al_2O_3 on Pt/Al_2O_3 catalyst in CO oxidation," *Catalysis Communications,* vol. 9, no. 4, pp. 546-550, 2008.

[15] K. Pansanga, J. Panpranot, O. Mekasuwandumrong, C. Satayaprasert, J. G. Goodwin, and P. Praserthdam, "Effect of mixed γ- and χ-crystalline phases in nanocrystalline Al_2O_3 on the dispersion of cobalt on Al_2O_3," *Catalysis Communications*, vol. 9, no. 2, pp. 207-212, 2008.

[16] S. Sujeerakulkai, and S. Jitkarnka, "Bio-based hydrocarbons and oxygenates from catalytic bio-ethanol dehydration: comparison between gallium and germanium oxides as promoters on HBeta zeolites with various silica to alumina ratios," *Journal of Cleaner Production*, vol. 111, pp. 51-61, 2016.

[17] B. K. Marcus, and W. E. Cormier, "Going Green with Zeolites," *Chemical Engineering Progress*, vol. 95, no. 6, pp. 47-53. 1999.

[18] J. Janlamool, and B. Jongsomjit, "Oxidative dehydrogenation of ethanol over AgLi–Al_2O_3 catalysts containing different phases of alumina," *Catalysis Communications,* vol. 70, pp. 49-52, 2015.

[19] G. Chen, S. Li, F. Jiao, and Q. Yuan, "Catalytic dehydration of bioethanol to ethylene over TiO_2/γ-Al_2O_3 catalysts in microchannel reactors," *Catalysis Today,* vol. 125, no. 1-2, pp. 111-119, 2007.
[20] J. Nowicki, L. Mokrzycki, and B. Sulikowski, "Synthesis of novel perfluoroalkylglucosides on zeolite and non-zeolite catalysts," *Molecules,* vol. 20, no. 4, pp. 6140-52, 2015.
[21] S. Hajimirzaee, M. Ainte, B. Soltani, R. M. Behbahani, G. A. Leeke, and J. Wood, "Dehydration of methanol to light olefins upon zeolite/alumina catalysts: Effect of reaction conditions, catalyst support and zeolite modification," *Chemical Engineering Research and Design,* vol. 93, pp. 541-553, 2015.
[22] H. Xin, X. Li, Y. Fang, X. Yi, W. Hu, Y. Chu, F. Zhang, A. Zheng, H. Zhang, and X. Li, "Catalytic dehydration of ethanol over post-treated ZSM-5 zeolites," *Journal of Catalysis*, vol. 312, pp. 204-215, 2014.
[23] X. Zhang, R. Wang, X. Yang, and F. Zhang, "Comparison of four catalysts in the catalytic dehydration of ethanol to ethylene," *Microporous and Mesoporous Materials,* vol. 116, no. 1-3, pp. 210-215, 2008.
[24] W. Alharbi, E. Brown, E. F. Kozhevnikova, and I. V. Kozhevnikov, "Dehydration of ethanol over heteropoly acid catalysts in the gas phase," *Journal of Catalysis,* vol. 319, pp. 174-181, 2014.
[25] Y. Han, C. Lu, D. Xu, Y. Zhang, Y. Hu, and H. Huang, "Molybdenum oxide modified HZSM-5 catalyst: Surface acidity and catalytic performance for the dehydration of aqueous ethanol," *Applied Catalysis A: General,* vol. 396, no. 1-2, pp. 8-13, 2011.
[26] T. K. Phung and G. Busca, "Ethanol dehydration on silica-aluminas: Active sites and ethylene/diethyl ether selectivities," *Catalysis Communications,* vol. 68, pp. 110-115, 2015.
[27] D. Liu, C. Yao, J. Zhang, D. Fang, and D. Chen, "Catalytic dehydration of methanol to dimethyl ether over modified γ-Al_2O_3 catalyst," *Fuel,* vol. 90, no. 5, pp. 1738-1742, 2011.
[28] C. Duan, X. Zhang, R. Zhou, Y. Hua, L. Zhang, and J. Chen, "Comparative studies of ethanol to propylene over HZSM-5/SAPO-34 catalysts prepared by hydrothermal synthesis and physical mixture," *Fuel Processing Technology,* vol. 108, pp. 31-40, 2013.